

Automatika

Journal for Control, Measurement, Electronics, Computing and Communications



ISSN: 0005-1144 (Print) 1848-3380 (Online) Journal homepage: <https://www.tandfonline.com/loi/taut20>

A robust controlling methodology for a grouting process

B. S. Zhang, G. C. Yan, J. Guo & J. Q. Guo

To cite this article: B. S. Zhang, G. C. Yan, J. Guo & J. Q. Guo (2020) A robust controlling methodology for a grouting process, *Automatika*, 61:1, 179-187, DOI: [10.1080/00051144.2019.1698190](https://doi.org/10.1080/00051144.2019.1698190)

To link to this article: <https://doi.org/10.1080/00051144.2019.1698190>



© 2019 The Author(s). Published by Informa UK Limited, trading as Taylor & Francis Group



Published online: 03 Dec 2019.



Submit your article to this journal [↗](#)



Article views: 225



View related articles [↗](#)



View Crossmark data [↗](#)



A robust controlling methodology for a grouting process

B. S. Zhang^{a,b}, G. C. Yan^a, J. Guo^{a,b} and J. Q. Guo^c

^aCollege of Mining Technology, Taiyuan University of Technology, Taiyuan, People's Republic of China; ^bShanxi Province Research Center of Green Mining Engineering Technology, Taiyuan, People's Republic of China; ^cKey Laboratory of In-Situ Property-Improving Mining of Ministry of Education, Taiyuan University of Technology, Taiyuan, People's Republic of China

ABSTRACT

The grouting technology is an effective and economic method in the grouting industry field. In this paper, a nonlinear model for the grouting dynamic process was established, and the controlling parameters were further modified through a robust method. Moreover, the grouting pressure system for the neural network was also modelled based on a sensitivity analysis algorithm, and in particular, the iterative learning algorithm and Lyapunov asymptotical theory. The results showed that such a robust controlling methodology was better than the normal manual operation method. The subsequent numerical simulations demonstrated that the tuning methodology could meet all the requirements for the grouting control with the maximum pressure variable in the range of 8.1%. The present study and the proposed method could be applied to various engineering projects and especially, to implement in the real control of damming grouting.

ARTICLE HISTORY

Received 27 July 2017
Accepted 20 November 2019

KEYWORDS

Modelling; robust control; grouting; dam foundation

1. Introduction

Grouting technology is an effective and economic method in the grouting industry field, which is often used to deal with the dam foundations, high buildings and highways. Grouting pressure is one of the key important parameters in the project of grouting dam. In order to improve mechanical properties of rock stratum, high pressure technique is popularly used in grouting projects [1]. In fact, the grouting pressure is double-edged for a grouting process. If the grouting pressure is too high, and dangerous crack extensions of rock mass [2] are superlative, the whole dam foundation will be uplifted and damaged [3]. As a result, it would lead to not only great losses in economics but also risks for the lives of peoples around a dam. Therefore, how to control reasonably the grouting pressure is one of the key points in the construction of dam grouting. At present, the tuning pressure online is heavily depended on specialist's experiences. Because the relationship of grouting pressure, grout flux and grouting density is complex and nonlinear, it is difficult for the engineers to control the grouting pressure accurately [4].

To improve the grouting operation level, all kinds of real-time data collection systems have been used in this field since the mid-1970s [5]. Many grouting monitoring systems have realized the data collection, data display online and geological information reports of grouting borehole. The three parameters grouting recorders

[6] have been widely used in grouting engineering for more observational information such as grouting pressure, grout flow and grout density. For example, the Analytical Instrument Association intelligent grouting system had been used successfully in a project at Hunting Run Dam. Grouting recorder significantly increased the accuracy and construction efficiency in grouting field, and operation risks have been reduced for engineers [7]. However, the above systems only can collect data, and the pressure is controlled by a manual operation because of its complexity. If pressure is up to 5 MPa, the control precision of manual operation is very low. It is difficult to grantee the accuracy if an engineer does not have rich experiences in the field.

In fact, early in 1990s, Zettler et al. [7] used the fuzzy intelligent system to control grouting stop time parameter based on project data, in which the operation experiences of the engineers were quantified as fuzzy rules. Then, there are some improvement methods about stopping grouting time. Fuzzy rules extraction method based on neural network learning was to solve the difficulty of extracting rules [8–11]. These studies show that the intelligent learning method is feasible for the grouting process based on macro-parameters of the grouting process [12–14]. The above researches are served to control grouting time. In the present work, the main objective is to automatically control the grouting pressure tracking on a design curve. The advanced research results of our team show that the back-propagation (BP)

neural model based on multi-sensor data technology can simulate the dynamic feature of the real grouting system [15].

Due to its simple structure, various old designs are still used widely as one of the most controllers for the grouting pressure in many industrial applications [16]. It is well known that the performance of a proportional-integral-derivative (PID) controller is mainly decided by its parameters. Garatti et al. [17] first proposed the tuning parameter of PID. Subsequently, many techniques have been developed and still research is going on for good and robust performance [18,19]. For example, the colony algorithm [20], such as particle swarm optimization (PSO) algorithm [21], was used to optimize the PID parameters. Furthermore, the self-learning PID control design has achieved huge success in theoretical researches and engineering applications. For example, Xue et al. used the reinforcement learning-based fuzzy PID to control load frequency of an island micro-grid [22]. Esmaili et al. proposed an immune learning algorithm for the PID controller design [23]. Rout and Wang et al. adopted an adaptive PID controller, which was developed using the derived parameters, to accomplish the path following task for an autonomous underwater vehicle [24]. For the complex problems, Rout and Subudhi proposed a collaborative optimal method [25]. Moreover, a speculative approach to solve multi-objective optimization in communication and cloudy environment [26,27] was also developed, where the PID gain tuning based on the data-driven iterative method could reach a good convergence [28].

In the present work, the concept of a robust Lyapunov error function combined with the iterative method to tune the PID controller and the dynamic system is described using an artificial neural network (ANN) model. In order to illustrate the utility of the presented technique, numerical simulations are performed in MATLAB based on the grouting field data. Hereafter, we collect data from the grouting field using a grouting recorder, and the ANN model was constructed based on the collected data. The input variable of the model is vital for model performance. Hence, a sensitivity analysis algorithm is adopted for choosing the input variables. On this basis, the valve will be automatically tuned by the PID controller according to the error between the measuring value and the design value. A new robust iterative algorithm of PID parameters is adopted in order to get more stable control precision.

The main contributions in the present work are two aspects. One contribution is to propose a nonlinear BP model of the grouting dynamic process. Another contribution is to modify the parameters of the PID controller through the robust method. The grouting model of the neural network is established by three steps. First, select the primary factors through the qualitative analysis of the dynamic grouting process. Second,

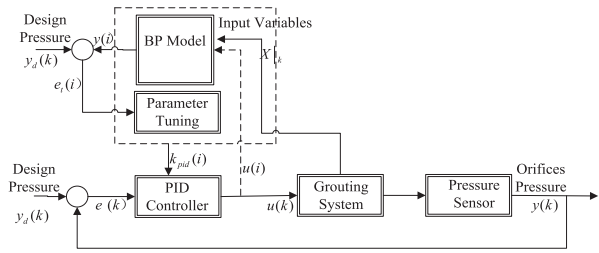


Figure 1. Grouting pressure control structure.

select quantitatively the input variables of the BP model based on the sensitivity analysis algorithm. At last, the BP model was trained and tested by new data in the field. The optimization of controller parameters was designed combining the iterative learning algorithm and Lyapunov asymptotical theory. PID gain matrix is updated iteratively according to the error between the neural network model online and the expected output value, which is obtained on each interval time step. The whole pressure control structure is shown in Figure 1.

2. Influence of the grouting pressure based on flow mechanism

In the grouting process, the cement grouts are injected into the crack of grouting hole through grouting barrel, pipe and pressure pump with high grouting pressure, as shown in Figure 2. The grouting monitoring system includes two flow sensors: one is pressure sensor, and another is density sensor. If the grouting pressure is higher than the design value, the engineer must tune the value quickly to decrease it.

Yokoyama and Masuda [29] proposed a macro-grouting pressure model

$$P_t = \frac{Lu}{0.98 \mu} \left(1 - \frac{\beta}{D_0} t\right)^3 \frac{1}{Q_t}, \quad (1)$$

where P_t is the grouting pressure at time t (MPa), Lu is Lugeon value of the grouting test (L/m/min), μ is the viscosity of the grouts, β is a constant value, a factor of injection rate (m/min), D_0 is the initial average crack width at $t = 0$ (m), t is the filling duration time (min), and Q_t is the grouts filled into rock crack at time t .

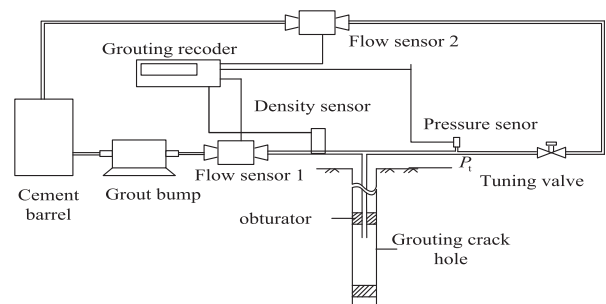


Figure 2. The basic structure of the cycle grouting system.

Table 1. The test value of different W/C ratios of grouts.

Number	W/C of grouts	Viscosity (mPa s)	Density (g/cm ³)
1	1:1	8.3	1.5
2	2:1	5.3	1.286
3	3:1	3.84	1.206

Based on the above grouting model, the factors influencing the grouting pressure include geological environments (Lugeon value and crack width), material properties of grouts and flow parameters.

According to the law of flow conservation of the grouting system, the injected flow Q_t is given as follows:

$$Q_t = Q_r - Q_2, \quad (2)$$

where Q_r is the grouts flow measured by flow sensor 1 in Figure 2, and Q_2 is grouts-back flow measured by flow sensor 2.

Assuming the valve opening and flow is linear, the pressure valve can be expressed as

$$\frac{Q_2}{Q_{\max}} = R \left(\frac{U_K}{U_{\max}} - 1 \right), \quad (3)$$

where Q_{\max} is the maximum flow rate of the regulating valve (100 L/min), U_{\max} is the largest adjustment opening, U_K is the adjustment opening value of the valve, and Q_2 is the grouts-back flow.

From Formula (2), the grouts-back flow Q_2 is proportion to the valve opening value $U(k)$. If we change the tuning valve, the grouts-back flow Q_2 is varied with it. According to Formulae (1) and (2), the grouting pressure will be varied with the grouts-back flow Q_2 . In the grouting field, Q_2 can be easily measured through the recorder, and $U(k)$ cannot be measured directly, so Q_2 is chosen as control variable.

The crack width cannot be measured for a dynamic grouting process. Although the relationship between grouting pressure and other parameters is nonlinear, the variations of crack conditions can be observed using other parameters such as grouting pressure, and flow velocity from paper [15].

In the grouting process, the ratio of water and cement of grouts has different requirements such as 1:1, 2:1 and 3:1. If the ratio is varied, the density (ρ) and viscosity are different (Table 1).

Based on the above simple analysis, the grouting pressure nonlinear model can be described as

$$P_G = f(\rho, \mu, Q_2, Q_t, Lu). \quad (4)$$

3. Selections of the input variables and model of the grouting system

3.1. Selections of the input variables based on the orthogonal test method

For the complex control process, the selection of input variable is a key factor for the "black-box" model. To

Table 2. Four factors and three levels.

Factors	Grouts density (g/cm ³)	Grouts viscosity (mPa s)	Grouts velocity (mm/s)	Lugeon value (L/min)
Level 1	1.5	8.3	98.6	5
Level 2	1.286	5.3	72.1	10
Level 3	1.206	3.84	26.5	15

simplify a model, the minor factors can be ignored. The orthogonal test method and augmented and hybrid approaches are universally used for the selection of major factors in a quantitative analysis method [30]. From Eq. (4), there are five factors related to the grouting pressure. Each factor has multi-levels. The orthogonal method can reduce the testing time and shorten the testing cycles [31]. In the test, the grouting hole can be setup as 15 m. Lugeon value (Lu) can be obtained from the water pressure test. The Grouts-back flow (Q_2) is closely related to Q_t from Eq. (2). With the help of four factors and three levels of the orthogonal table, nine orthogonal experiments were designed to study the influences of grouts density and viscosity, inlet grouts flow and Lugeon value on the performance of grouting pressure. The levels of each parameter were determined by selecting some typical values. Three levels of grouts density were 1.5, 1.286 and 1.206 g/cm³, respectively. The three levels of grouts viscosity were 8.3, 5.3 and 3.84 mPa s, respectively. The three levels of inlet grouts velocity were 98.6, 72.1 and 26.5 mm/s, respectively. The three levels of the Lugeon value were 5, 10 and 15 L/min, respectively. These factors and their corresponding levels are shown in Table 2.

The orthogonal design with four factors and three levels formed is shown in Table 3.

The grouting density, grouts flow and grouting pressure can be recorded using the grouting system (Figure 3).

All tests were carried out according to Table 3. The deviation of grouting pressure and design value was adopted as statistical data. The deviation of grouting pressure is shown in Table 4. According to the orthogonal experiments, the range analysis was conducted using a statistical method [31,32] to determine the sensitivity of various factors to the grouting pressure. The performance index was the statistical extreme value. The greater the extreme value was, the more sensitive the factor was. The calculation process for the range analysis is shown as follows:

$$S_{XM} = I_{XM} - Y, \quad (5)$$

$$R_{0X} = \text{MAX}(S_{X1}, S_{X2}, S_{X3}), R_{1X} \\ = \text{MIN}(S_{X1}, S_{X2}, S_{X3}), \quad (6)$$

$$G_X = R_{0X} - R_{1X}, \quad (7)$$

where S_{XM} stands for the average value of the experimental results, which contain the factor X with m level. Y stands for the average value of all the test results.

Table 3. Grouting process orthogonal design.

Test number	Grouts density (g/cm ³)	Grouts viscosity (mPa s)	Grouts velocity (mm/s)	Lugeon value (L/min)	Output pressure (kPa)
1	1.5	8.3	98.6	5	50.4
2	1.5	5.3	72.1	15	315.8
3	1.5	3.84	26.5	10	507.3
4	1.286	8.3	72.1	10	53.4
5	1.286	5.3	26.5	5	313
6	1.286	3.84	98.6	15	500.9
7	1.206	8.3	26.5	15	52.4
8	1.206	5.3	98.6	10	312.9
9	1.206	3.84	26.5	5	500.5

**Figure 3.** Grouting test system.**Table 4.** The calculation results of the orthogonal experiment.

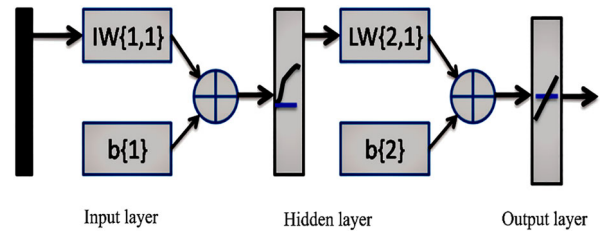
Factors	Levels			G_X
	1	2	3	
A	$S_{A1} = 9.04$	$S_{A2} = 2.94$	$S_{A3} = 1.54$	7.5
B	$S_{B1} = 3.74$	$S_{B2} = 3.54$	$S_{B3} = 6.24$	2.7
C	$S_{C1} = 0.14$	$S_{C2} = 5.24$	$S_{C3} = 8.34$	8.2
D	$S_{D1} = -0.26$	$S_{D2} = 8.94$	$S_{D3} = 4.84$	9.2

Thus, S_{XM} reflects the difference between the average value of the experimental results and the average value of all the test results. I_{XM} stands for the influence of the factor X. If G_X value is high, the influence of X is great. The calculation results are shown in Table 4.

In Table 4, A, B, C and D are grouts density, grouts viscosity, grouts velocity and Lugeon value, respectively. From Table 4, it can be concluded that $G_X(D) > G_X(C) > G_X(A) > G_X(B)$, implying that the effects of the Lugeon value on the performance of the control system is the largest whereas the effect of grouts viscosity is the least.

3.2. The black model of the grouting system-based BP model

For a mathematical model of the grouting process, the dynamic performance should be described properly. A grouting system is uncertain and complex, so its control system is not described as the transfer function. A grouting pressure is nonlinear with grouts injected flow and density. The BP neural network has a capability to fit the nonlinear mapping relation between the input

**Figure 4.** Structure of the BP model of the grouting system.

and the output. In order to identify and predict the non-linear property of grouting pressure, we propose a BP neural model based on multi-sensor data offline.

Based on the above analysis in Section 3.1, we choose Lugeon value, such as grouting velocity (grouts flow), grouts density as the input variables X, and $y(k) = P_G(K)$ as the output variable. For the BP model, three inputs and one output are needed. The layer numbers and transfer function can be got through the BP learning where the trial method can be used. The grouting system model is described in Figure 4.

The BP model modifies the transferring function and parameters based on the principle of minimization of errors. The error evaluation index is expressed as

$$MSE(x_i) = \frac{1}{l} \sum_{i=1}^l (f(x_i) - y_i)^2, \quad (8)$$

where l is the sampling set number, $f(x_i)$ is the output of the model, and y_i is the experimental value.

The grouting system is shown in Figure 3, which can collect the field data of Lugeon value, grouts flow, grouts density and output grouting pressure. We can use field data to supervise the learning process. Data were collected on the Shubuta dam project in China and are shown in Figures 5–7. The Lugeon value of the grouting test is 2.1–3.6.

The BP model algorithm includes three parts:

- (1) Collections of variable data and normalization. Data normalization is performed in order to eliminate the influence from the wide-ranging data on the model; the formula is

$$y_{\min} = 0, y_{\max} = 1, y = (y_{\max} - y_{\min}) * (x - x_{\min}) / (x_{\max} - x_{\min}) + y_{\min}. \quad (9)$$

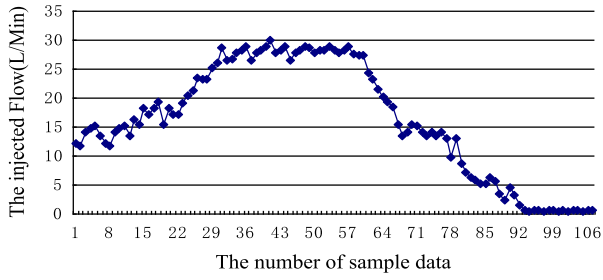


Figure 5. The field injected flow data on the grouting data.

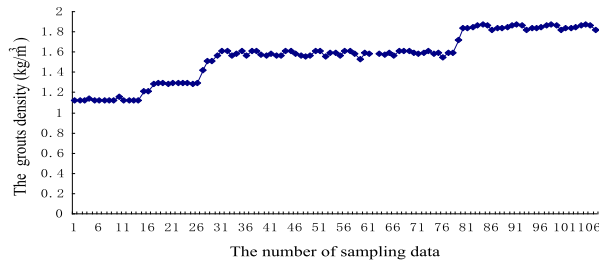


Figure 6. The field grouts density data on the grouting data.

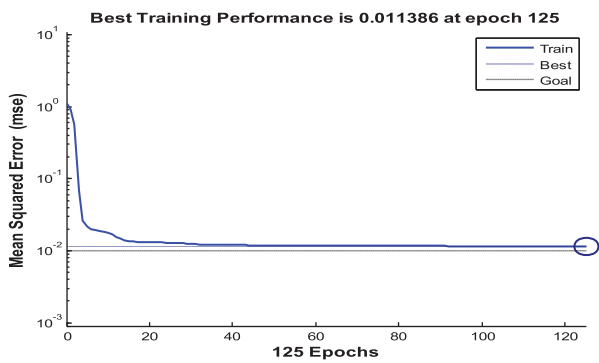


Figure 7. The training performance of MSE.

- (2) Training of the BP model based on the part above data sets. The training process is repeated over several cycles (epochs) to reduce the error between predicted and target values, which include tuning the hidden layers numbers, transferring function and other model parameter set. To minimize objective error, the Levenberg–Marquardt BP optimization is used. Training is stopped when one of the defined goals is reached, minimizing mean square error (MSE) over a reasonable amount of time. All the parameters are shown in Table 5. The model MSE is shown in Figure 7.
- (3) Testing of the model using new data sets. Use the new data to test the model performance based on the test data set. The simulation result of the dynamic grouting process is shown in Figure 8. The MSE is 0.013734 at epoch 250. The picture result proves that the BP model can simulate the nonlinear of the real grouting system.

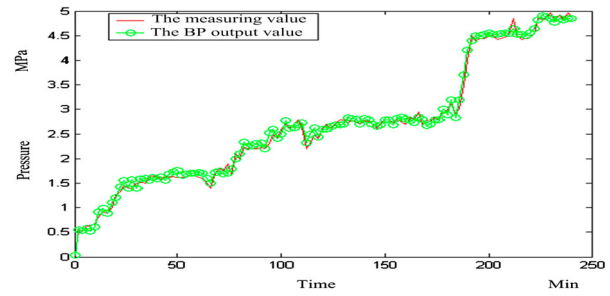


Figure 8. The test performance of the BP model.

Table 5. The training model parameter.

Parameters	
Data number	79
Hidden layers	5
Output layer	1
Hidden-layer function	Tagsig
Output layer function	Purelin
Training algorithm	Levenberg–Marquardt

4. A robust tuning method of the PID parameters based on the BP model

Although many advanced control approaches have been proposed, PID controllers are widely used in the industrial feedback process for its simple structure [32,33]. However, the main problem of the PID controller is the tuning parameters for higher perfect characters. Over the past years, many tuning methods such as optimal PSO [34], fuzzy tuning [35] and model-based optimal method [36,37] were developed. For a grouting system, the maximum pressure must be controlled dynamically. For a better ability, a robust iterative algorithm was adopted based on tracking errors. The discrete PID is

$$u(k) = k_p(k)e(k) + k_i(k) \sum_{i=0}^k e(i) + k_d(k) \frac{e(k) - e(k-1)}{T}, \quad (10)$$

where $e(k) = y_d(k) - y(k)$ is the tracking error, $y_d(k)$ and $y(k)$ are desired value and system output, T is the sampling time, $k_p(k)$, $k_i(k)$, $k_d(k) \in R^{m \times p}$ are PID tuning parameter matrix, and m is the number of input variable.

For obtaining the optimal parameters $k_p(k)$, $k_i(k)$, and $k_d(k)$, a matrix for multi-input variables can be expressed as

$$\theta_{pid}(k) = \begin{bmatrix} [k_{p1}(k) & k_{i1}(k) & k_{d1}(k)]^T \\ [k_{p1}(k) & k_{i1}(k) & k_{d1}(k)]^T \\ \vdots \\ [k_{pm}(k) & k_{im}(k) & k_{dm}(k)]^T \end{bmatrix}, \quad (11)$$

where $k_{pj}(k)$, $k_{ij}(k)$, and $k_{dj}(k)$ are the row values $k_p(k)$, $k_i(k)$, and $k_d(k)$, $j = 1, 2, \dots, m$.

The controller will find the optimal parameters at each time k through iterative for the least tracking error. Therefore, the parameters maybe tuned at different sampling; i is described as the iterative steps in the sample period. The variables at k are described as $|_k$, for example, $\theta_{pid}(k) \rightarrow \theta_{pid}|_k$.

The optimal PID $\theta_{pid}(k)$ is obtained by iterative computing. $\hat{\theta}_{pid}(i)$ is the estimation variables in the i step time. The tuning algorithm of PID parameters is

$$\hat{\theta}_{pid}(i+1) = \hat{\theta}_{pid}(i) + \Delta\hat{\theta}_{pid}(i) = \hat{\theta}_{pid}(i) + k_{pid}(i)e_t(i), \quad (12)$$

where $k_{pid}(i)$ is the gain matrix, $e_t(i)$ is the nominal error of design value and ANN output value at time i , which is not the system error $e_t(k)$. $e_t(i)$ can be expressed as

$$e_t(i) = y_d|_k - \hat{y}(i), \quad (13)$$

where $y_d|_k$ is the desired output at k time, and $\hat{y}(i)$ is the ANN output at i step.

$\hat{y}(i)$ can be described as

$$\hat{y}(i) = \hat{g}[\hat{u}(i), X|_k],$$

where $\hat{u}(i)$ is the nominal optimal value, and $\hat{u}(i)$ is described as

$$\hat{u}(i) = K_p(i)e|_k + K_i(i)E_{pid}|_k + K_d(i)\frac{e|_k - e|_{k-1}}{T}. \quad (15)$$

The discrete Lyapunov function of the output error is

$$V(i) = \delta e_t(i)^T e_t(i), \quad (16)$$

where δ is a positive constant, obviously, and $V(i)$ is positive definite.

$$e_t(i) = e_t(i-1) + \Delta e_t(i-1). \quad (17)$$

In a discrete system, a small increment variable can be looked as the similarity of the first-order derivative of error function. $\Delta\hat{\theta}_{pid}(i)$ is similar to the derivative function. $y_d|_k$ can be thought as a constant value at time i , and as a result, their partial derivative value is zero. $\Delta e_t(i)$ can be described as

$$\begin{aligned} \Delta e_t(i) &= \frac{\partial e_t(i)}{\partial \hat{\theta}_{pid}(i)} \frac{\partial \hat{\theta}_{pid}(i)}{\partial(i)} = \frac{\partial [y_d|_k - \hat{y}(i)]}{\partial \hat{\theta}_{pid}(i)} \Delta \hat{\theta}_{pid}(i) \\ &= -\frac{\partial \hat{y}(i)}{\partial \hat{\theta}_{pid}(i)} k_{pid}(i) e_t(i). \end{aligned} \quad (18)$$

The increment value of the Lyapunov function is expressed as

$$\begin{aligned} \Delta V(i) &= V(i+1) - V(i) \\ &= 2\delta \Delta e_t(i)^T [e_t(i) + \delta \Delta e_t(i)] \\ &= -2\delta \left[\frac{\partial \hat{y}(i)}{\partial \hat{\theta}_{pid}(i)} k_{pid}(i) e_t(i) \right]^T \\ &\quad \times \left[e_t(i) - \delta \frac{\partial \hat{y}(i)}{\partial \hat{\theta}_{pid}(i)} k_{pid}(i) e_t(i) \right] \\ &= -2\delta e_t(i)^T \left[\frac{\partial \hat{y}(i)}{\partial \hat{\theta}_{pid}(i)} k_{pid}(i) \right]^T \\ &\quad \times [I - \delta] \left[\frac{\partial \hat{y}(i)}{\partial \hat{\theta}_{pid}(i)} k_{pid}(i) \right] e_t(i). \end{aligned} \quad (19)$$

The gain matrix $k_{pid}(i)$ is

$$k_{pid}(i) = \frac{1-\delta}{\delta} \left[\frac{\partial \hat{y}(i)}{\partial \hat{\theta}_{pid}(i)} \right]^T \left\{ \frac{\partial \hat{y}(i)}{\partial \hat{\theta}_{pid}(i)} \left[\frac{\partial \hat{y}(i)}{\partial \hat{\theta}_{pid}(i)} \right]^T \right\}. \quad (20)$$

Then, $\Delta V(i)$ is

$$\Delta V(i) = -2(1-\delta) e_t(i)^T e_t(i). \quad (21)$$

Jacobian matrix of Formula (14) can be described as

$$\frac{\partial \hat{y}(i)}{\partial \hat{\theta}_{pid}(i)} = \frac{\partial \hat{y}(i)}{\partial \hat{u}(i)} \frac{\partial \hat{u}(i)}{\partial \hat{\theta}_{pid}(i)}. \quad (22)$$

Related to the ANN model

$$\begin{aligned} \frac{\partial \hat{y}(i)}{\partial \hat{u}(i)} &= \frac{\partial \hat{y}(i)}{\partial o(i)} \frac{\partial o(i)}{\partial z(i)} \frac{\partial z(i)}{\partial \hat{u}(i)} \\ &= \frac{\partial W^y \begin{bmatrix} o(i) \\ 1 \end{bmatrix}}{\partial o(i)} \begin{bmatrix} \frac{\partial o_1(i)}{\partial z_1(i)} & \cdots & 0 \\ \vdots & \ddots & \vdots \\ 0 & \cdots & \frac{\partial o_q(i)}{\partial z_q(i)} \end{bmatrix} \\ &\quad \times \frac{\partial W^h \begin{bmatrix} \hat{u}(i) \\ X|_K \\ 1 \end{bmatrix}}{\partial \hat{u}(i)} \\ &= \begin{bmatrix} W_{1,1}^y & \cdots & W_{1,m}^y \\ \vdots & \ddots & \vdots \\ W_{q,1}^y & \cdots & W_{q,m}^y \end{bmatrix} \\ &\quad \times \begin{bmatrix} \frac{\partial o_1(i)}{\partial z_1(i)} & \cdots & 0 \\ \vdots & \ddots & \vdots \\ 0 & \cdots & \frac{\partial o_q(i)}{\partial z_q(i)} \end{bmatrix} \\ &\quad \times \begin{bmatrix} W_{1,1}^h & \cdots & W_{1,m}^h \\ \vdots & \ddots & \vdots \\ W_{q,1}^h & \cdots & W_{q,m}^h \end{bmatrix}, \end{aligned} \quad (23)$$

where

$$\frac{\partial o_j(j)}{\partial z_j(i)} = o_j(j)[1 - o_j(j)], \quad j = 1, \dots, q,$$

$$z(i) = W^h \begin{bmatrix} \hat{u}(i) \\ X|_K \\ 1 \end{bmatrix}.$$

The partial derivative $\hat{u}(i)$ to $\hat{\theta}_{pid}(i)$ is described as

$$\begin{aligned} \frac{\partial \hat{u}(i)}{\partial \hat{\theta}_{pid}(i)} &= \frac{\partial \left[k_p(i)e|_k + k_i(i) \sum_{i=0}^k e|_k + k_d(i) \frac{e|_k - e|_{k-1}}{T} \right]}{\partial \hat{\theta}_{pid}(i)} \\ &= \begin{bmatrix} Q_{pid} & \dots & 0_{1 \times 3} \\ \vdots & \ddots & \vdots \\ 0_{1 \times 3} & \dots & Q_{pid} \end{bmatrix}, \end{aligned} \quad (24)$$

where

$$Q_{pid} = \begin{bmatrix} e_t|_k \\ \sum e_t|_k \\ \frac{e_t|_k - e_t|_{k-1}}{T} \end{bmatrix}.$$

Through the above analysis, the gain matrix $k_{pid}(i)$ can be obtained from (20), and $\hat{\theta}_{pid}(i)$ can asymptotically converge to the optimal value. As a result, the tracking error will be stable.

5. Simulation results for the grouting process

In a grouting process, pressure control can be divided into two types. One is that the pressure is kept as a constant, even if the grout density and flow are fluctuated. Such a system can maintain a constant pressure through continuous sampling to rhw BP model and can achieve control parameters based on the above robust method and the PID adjuster by operating the output pipe valve part. Another is that the grouting pressure is setup as a step function since it increases from low to high state. If a grouting zone rock is relative integrity, one can usually increase the grouting pressure directly. However, if the rock conditions are poor, the pressure can be increased

by three step changes and even more steps. In order to demonstrate the application of the robust ANN-based PID tuning methodology proposed in this paper, we now present the simulation results based on the field monitoring data for a grouting process performed using the MATLAB. For the above method, first a model of the grouting process should be established, and then the PID parameters in each discrete time K should be tuned based on the model error and design value.

The grouting mathematical model was first proposed based on input–output data offline in Section 3.2. $x_3 = \{Q_t, Lu, \rho\}$ was the input variable for the BP model, the grouting pressure at grouts-back hole pipe was the output variable. The control variable was valve opening, which can be substituted with the grouts-back volume flow.

After obtaining the ANN model, the PID parameters using the method in Section 4. The first test is keeping grouting pressure at a constant of 2.5 MPa, with the density of grouting ranged from 1.18 to 1.76 kg/m³. The control results are shown in Figure 9.

The second test is to show the robustness of the proposed method compared to the different flow disturbances. The grouting pressure in the proposed method can be steady in 3 min even if there are 10% flow disturbances. If the flow disturbances reach 20% to the maximum of real flow, it still can exhibit a good convergence property. As a result, the grouting pressure can be steady in 5 min. Here, it is noted that in the real project, the flow disturbances is within 20% of the maximum value (Figures 10 and 11).

The other tests are to increase grouting from 0.5 to 4.5 MPa, with flow Q_t ranged from 10 to 50 L/min, Lu ranged from 0.5 to 0.8 L/m/min and the density of grouting ranged from 1.18 to 1.76 kg/m³. The dynamic pressure with the robust control method is shown in Figure 12. In this system, the grouting pressure is below the maximum design, implying that the proposed method can be applied to a real engineering project for its convergence.

Finally, we compared our results to a common optimal method such as an improved adaptive PSO (APSO)

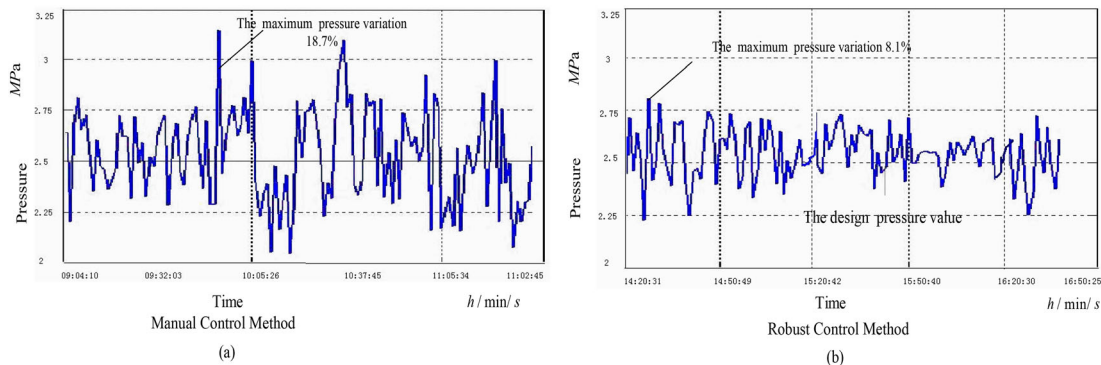


Figure 9. The control performance contraction with the manual and robust control method at 2.5 MPa.

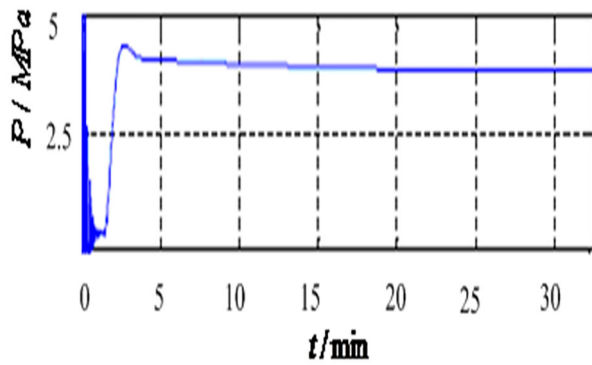


Figure 10. The output pressure in 10% flow disturbances.

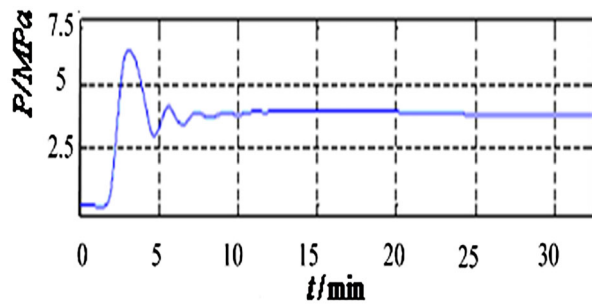


Figure 11. The output pressure in 20% flow disturbances.

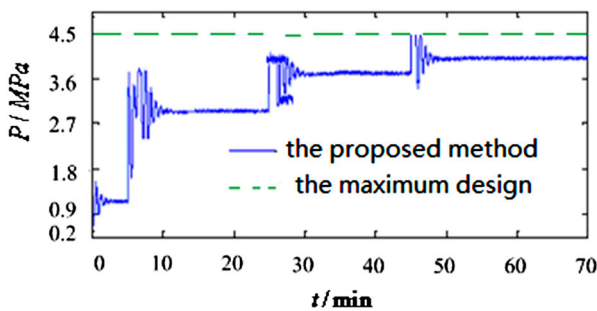


Figure 12. The control performance contraction with the robust control method from 0.5 to 4.5 MPa.

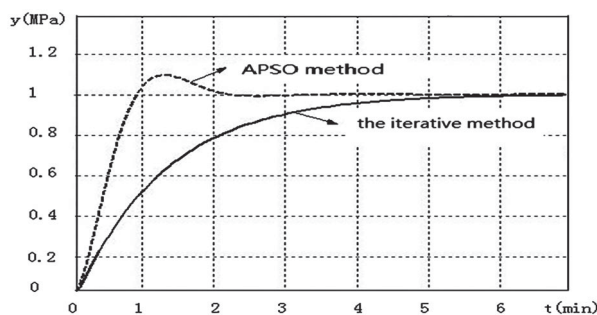


Figure 13. The step response in different optimal tuning methods.

algorithm in Ref. [15]. The comparison is shown in Figure 13. As seen, the grouting system can hardly show an acute fluctuation. Here, it should also be indicated that the real grouting pressure cannot reach the designed maximum value, implying that the iterative method is better than the APSO method.

6. Summary

A robust controlling methodology of the PID controller for a pressure grouting system has been developed by combining the ANN model and the iterative technique. The results show that the present tuning methodology can meet the requirement of grouting control with the maximum pressure variable in the range of 8.1%, which can attenuate the transient vibration of pressure for the variations of grouting density and flow velocity. Furthermore, the proposed method can reduce the fluctuation of density and flow in different stages, and the whole dynamic grouting is stable and below the maximum design value. Moreover, the comparison between two different optimal methods demonstrates that the proposed iterative method is more stable and more secure for tuning the parameters of the PID. Additionally, it is revealed that the pressure transient surge is very harmful to the grouting project, leading to the broken grouting pipe and the lifted rock mass.

Acknowledgements

This work was supported by the Transformation of Scientific and Technological Achievements Programs of Higher Education Institutions in Shanxi (grant number JYT2019015).

Disclosure statement

No potential conflict of interest was reported by the authors.

References

- [1] Rafi JY, Stille H. Control of rock jacking considering spread of grout and grouting pressure. *Tunnelling Underground Space Technol.* 2014;40(2):1–15.
- [2] Yuan H, Cao P, Xu W. Mechanism study on sub-critical crack growth of flabby and intricate ore rock. *Trans Nonferrous Metals Soc China.* 2006;16(3):723–727.
- [3] Xiao GG, Shaorong C. Study on lift control of toe-plate grouting of high Concrete-Faced Rockfill Dam. *J Yangtze River Sci Res Inst.* 2006;23(3):23–24.
- [4] Gustafson G, Claesson J, Fransson Å. Steering parameters for rock grouting. *J Appl Math. (Special Issue).* 2013;32(3):337–366.
- [5] Li XU, Chen W, Peng HY, et al. Spot calibration and parameter error analysis of measurement and control system for grouting and water permeability tests. *Water Resources & Hydropower Engineering;* 2004.
- [6] Zhong DH, Yan FG, Li MC, et al. A real-time analysis and feedback system for quality control of dam foundation grouting engineering. *Rock Mech Rock Eng.* 2014;48(5):1–22.
- [7] Zettler AH, Poisel R, Reichl I, et al. Pressure sensitive grouting (PSG) using an artificial neural network combined with fuzzy logic. *Int J Rock Mech Mining Sci.* 1997;34(3):358.e1–358.e14.
- [8] Alfi A, Khooban MH, Abadi DNM. Control of a class of non-linear uncertain chaotic systems via an optimal type-2 fuzzy proportional integral derivative controller. *IET Sci Meas Technol.* 2013;7(1):50–58.
- [9] Soltanpour MR, Khooban MH. A particle swarm optimization approach for fuzzy sliding mode control

- for tracking the robot manipulator. *Nonlinear Dyn.* **2013**;74(1-2):467-478.
- [10] Niknam T, Khooban MH, Kavousifard A, et al. An optimal type II fuzzy sliding mode control design for a class of nonlinear systems. *Nonlinear Dyn.* **2014**;75(1-2):73-83.
- [11] Khooban MH, Abadi DNM, Alfi A, Siah M. Optimal type-2 fuzzy controller for HVAC systems. *Automatika.* **2014**;55(1):69-78.
- [12] Khalghani MR, Shamsi-Nejad MA, Khooban MH. Dynamic voltage restorer control using bi-objective optimisation to improve power quality's indices. *IET Sci Meas Technol.* **2014**;8(4):203-213.
- [13] Khalghani MR, Shamsi-Nejad MA, Farshad M, et al. Modifying power quality's indices of load by presenting an adaptive method based on Hebb learning algorithm for controlling DVR. *Automatika.* **2014**;55(2):153-161.
- [14] Abadi DNM, Khooban MH. Design of optimal Mamdani-type fuzzy controller for nonholonomic wheeled mobile robots. *J King Saud Univ Eng Sci.* **2015**;27(1):92-100.
- [15] Li FL, Shen QT, Xu LS. Nonlinear model predictive pressure for grouting system. *J Syst Simul.* **2008**;20(23):6535-6506.
- [16] Ziegler JG, Nichols NB. Optimum settings for automatic controllers. *Trans ASME.* **1942**;64:759-768.
- [17] Garatti S, Campi MC, Bittanti S. Iterative robust control: speeding up improvement through iterations. *Syst Control Lett.* **2010**;59(2):139-146.
- [18] Suzuki A, Sugimoto K. Robust PID parameter design for embedded temperature control system using Taguchi method. *IEEE Trans Sens Micromach.* **2006**;126(12):1660-1666.
- [19] Verboven S, Hubert M. LIBRA: a MATLAB library for robust analysis. *Chemom Intell Lab Syst.* **2005**;75(2):127-136.
- [20] Satoh H, Yamaguchi Y, Abe T. Investigation on dam foundation grouting process. *J Jpn Soc Dam Eng.* **2005**;19(2):384-391.
- [21] Heidelberg SB. *Cement grouting.* Berlin: Springer; **2014**.
- [22] Xue Y, Jiang JM, Zhao BP, et al. A self-adaptive artificial bee colony algorithm based on global best for global optimization. *Soft Comput.* **2017**. DOI:10.1007/s00500-017-2547-1
- [23] Esmaeili M, Shayeghi H, Nejad HM, et al. Reinforcement learning based PID controller design for LFC in a micro-grid. *Compel Int J Comput Math Electr.* **2017**;36(4):34-39.
- [24] Wang M, Feng S, He C, et al. An artificial immune system algorithm with social learning and its application in industrial PID controller design. *Math Probl Eng.* **2017**;5(3):1-13.
- [25] Rout R, Subudhi B. Inverse optimal self-tuning PID control design for an autonomous underwater vehicle. *Int J Syst Sci.* **2017**;48(2):367-375.
- [26] Deng W, Zhao H, Yang X, et al. Study on an improved adaptive PSO algorithm for solving multi-objective gate assignment. *Appl Soft Comput.* **2017**;59:288-302.
- [27] Deng W, Zhao H, Zou L, et al. A novel collaborative optimization algorithm in solving complex optimization problems. *Soft Comput.* **2017**;21(15):4387-4398.
- [28] Liu Q, Cai W, Shen J, et al. A speculative approach to spatial-temporal efficiency with multi-objective optimization in a heterogeneous cloud environment. *Security Commun Netw.* **2016**;9(17):4002-4012. DOI:10.1002/sec.1582
- [29] Yokoyama R, Masuda S. Convergence property for iterative data-driven PID gain tuning based on generalized minimum variance regulatory control. *International symposium on advanced control of industrial processes; 2011 Feb 21; Gaithersburg, USA.* IEEE; **2017**.
- [30] RenJie L. Orthogonal test design for optimization of the extraction of polysaccharides from *Phascolosoma esulenta* and evaluation of its immunity activity. *Carbohydr Polym.* **2008**;73(4):558-563.
- [31] Pengfei AI, Shan SU, Jin Z. Optimization of SRAP-PCR system on *Glycyrrhiza uralensis* by orthogonal test design and selection of primers. *Hebei J Ind Sci Technol.* **2017**;15:23-28.
- [32] Xu YH, Shen R, Liu DJ, et al. Optimizing the extraction process of chlorogenic acid and loganin in *Caulis Lonicerae* by orthogonal test method. *J Shantou Univ Med Coll.* **2017**;12:143-151.
- [33] Gao X, Zhang Y, Zhang H, et al. Effects of machine tool configuration on its dynamics based on orthogonal experiment method. *Chin J Aeronaut.* **2012**;25:285e91.
- [34] Xu Y, You T, Du C. An integrated micromechanical model and BP neural network for predicting elastic modulus of 3-d multi-phase and multi-layer braided composite. *Compos Struct.* **2015**;122:308-315.
- [35] Zhou YT, Nie JB, Han N, et al. Study on PID parameters tuning based on particle swarm optimization. *Adv Mat Res.* **2013**;823:432-438.
- [36] Xiao-Kan W, Zhong-Liang S, Wanglei, et al. Design and research based on fuzzy PID-parameters self-tuning controller with MATLAB. *International Conference on Advanced Computer Theory and Engineering; 2014 Aug 23; Beijing, China.* **2008**. p. 996-999.
- [37] Glavan M, Gradišar D, Atanasijević-Kunc M, et al. Input variable selection for model-based production control and optimisation. *Int J Adv Manuf Technol.* **2013**;68(9):2743-2759.